# Low Power Hydrometry for Open Channel Flows

Zahoor Ahmad, Abubakr Muhammad
Department of Electrical Engineering, SBA School of Science & Engineering, LUMS,
Lahore, Pakistan
zahoor.ahmad@lums.edu.pk, abubakr@lums.edu.pk

***Abstract*—Inspired by the need to monitor and control the world's largest irrigation and river networks such as those in the Indus River Basin, we have developed a smart water meter to gauge open channel flows. While developing this design, we have overcome challenges related to power consumption, precision, accuracy, calibration, field conditions, data communication and cost. Large scale deployment of such WSN inspired meters will ensure equity of water distribution, better management opportunities and hence reduce water scarcity.**

***Keywords*—telemetry; water meter; GPRS; ultrasonic**

## I. Introduction

Many river systems and irrigation networks around the world require unprecedented levels of automation and usage of decision support systems to enhance system health and ensure high efficiencies of water delivery. Frequent and pervasive measurement of open channel flows is one basic requirement for such automation. In many developing countries, where the need for such large-scale deployment is the highest, the desire for infrastructure modernization conflicts with economic constraints on both deployment and maintenance. Therefore, there is a need to develop extremely low-cost, low-maintenance and scalable open channel flow measurement systems. As in [13], the authors give an overview of such a system being developed and deployed for irrigation networks in Pakistan. The work is part of a wider research initiative, to determine the feasibility of a fully automated, smart water grid for Pakistan covering other aspects of estimation, control, optimization and decision making [6], [9]. The initiative is strongly linked with issues related to participatory irrigation management, enforcement of water rights and accountability. As in [10], a similar work carried out by ABB. This system described in [11] focuses on automating the hourly-to-daily measurement of canal water discharges in the network. In this paper, we give full details of the electronics designed for a wireless sensor network (WSN) technology inspired flow gauge, most suitable for installation on branch canals and distributaries at irrigation canal networks in a developing world scenario. In this paper, we report issues related to design, performance and calibration of the WSN node. We discuss steps to achieve extremely low-power battery powered design providing a practical compromise between two extremes: A direct AC mains powered system which is infeasible at remote locations and a solar-powered system which is difficult to secure physically and adds significantly to the cost. Our design guarantees a long-life completely battery powered system only requiring low-cost annual battery replacement. Secondly, we successfully demonstrated usage of maintenance-free ultrasound based sensing instead of conventional mechanical floats or pressure transducers. We have selected extremely accurate, weather proof and narrow beam sensors to overcome installation difficulties within a stilling well. We have taken care to compensate for changes in speed of sound in weather exposed conditions. Thirdly, the unit is field deployable in that we have packaged, tested and calibrated the sensor for all extreme conditions.

## II. Hardware Architecture

Refer to the block diagram shown in Fig. 1. The nine blocks represents the main components of the hardware.The microcontroller, PIC18F26K20 works as a master component, controlling the state of most of the modules. As, the sensors, we use in our application are not consuming more than 2mA of current, so we are making them on/off through microcontroller pin. We make them for less than one second, during sampling time. Real time clock (RTC) is run by a separate 3.3V cell. Battery is directly connected to GPRS module, but we are making it on/off using PWRKEY pin of SIM900D. The MCU has three wire connection with the GPRS module i.e., asynchronous transmit/receive and PWRKEY pin. Refer Fig. 2 for the photographs of the developed meter.

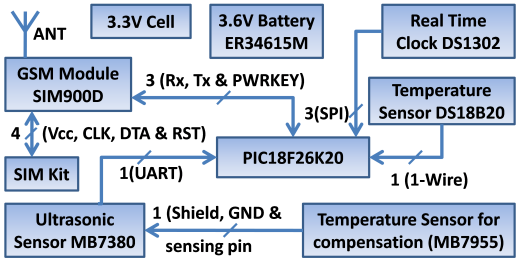


Fig. 1: Block diagram of wireless sensor node.

Fig. 2: Photographs of the developed smart water meter.

### A. Ultra Sonic Sensor

The Maxbotix MB7380 Ultra Sonic Sensor [3] is a cost-effective solution for applications where precision range-finding, low voltage operation, low-cost and IP67 weather resistance rating is needed. This sensor line features 1-mm resolution. The manufacturer claims to have an accuracy of 1%. So for a target distance of 1 meter it would be approximately 10mm. If the temperature or applied voltage changes during sensor operation, the sensor will apply necessary temperature and voltage compensations. Although the MB7380 has an internal temperature sensor; for best accuracy, we used the optional external temperature sensor MB7955 for compensation. MB7380 sensor has a calibrated beam pattern. Beam pattern is a 2D representation of the detection area of the sensor. The beam pattern is actually shaped like a 3D cone. Refer to Fig. 3 for beam pattern on 30 cm grid. Generally, for shorter distances we need narrower beam angle. Our expected distance to be measured is 1-2 meters. Stilling wells are designed across the canals, where these water meters are installed. The dotted lines indicate the boundaries of the stilling well. The dimensions of stilling well are 60cm*90cm, so it is clear from Fig. 3 that the cone does not interfere with the walls of the stilling well.

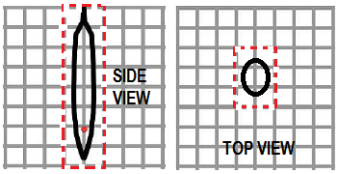


Fig. 3: Approximate beam pattern inside the stilling well on 30 cm grid.

### B. Microcontroller

Microchip's PIC18F26K20 flash microcontroller [4] with extreme low power (XLP) is used in our embedded design with 1.8V to 3.6V operating range. It is featured with up to 64 kbytes of linear program memory addressing, 1024 bytes of EEPROM data and up to 3936 bytes linear data memory addressing. Each data sample is time stamped which makes it 8 bytes long. We save the most recent 110 records in non-volatile EEPROM and the remaining 400 records in the volatile SRAM. If we have 24 records daily. Thus, with this much SRAM, we can save 16 days data in case of GPRS/GSM transmission problems and in case of power problem we can save up to 4 days data. Unlike other Microchip's MCUs, the EEPROM memory write/erase endurance of PIC18F26K20 is limited to 10k cycles, due to silicon issues [5]. Hence, while programming, we avoided using erase/write cycles frequently. The choice of this MCU is due to its high memory (programming memory, EEPROM and SRAM) and its Fixed Voltage Reference (FVR) module. As WSN turns on, MCU reads all EEPROM locations (100 records) and send them in the first transaction. In normal transactions, our message is limited to 50 records. In case of continuous previous GPRS transactions failure, if successfully connected, it sends all the data it has on volatile RAM (400 records) in eight different connections. The circuit has a 5 pin In Circuit Serial Programming (ICSP) connector. We are using PICKIT 3 for its ease of programming even in the field.

### C. GPRS/GSM Module

SIM900d is an ultra-compact and reliable wireless module-SIM900D. This is a complete Quad-band GSM/GPRS module [8] in a SMT type and designed with a very powerful single-chip processor integrating AMR926EJ-S core, which makes it cost-effective and small in dimensions. The module is integrated with the TCP/IP protocol. SIM900d has GPRS data and transfer of 42.8 kbps, RF output power is around 33dBm and RF receive sensitivity is around -107dBm. Refer to Fig. 4 for SIM card interface with SIM900d. The module automatically detects whether to provide 1.8V or 3.0V to the SIM card. SIM card is powered from internal 3.0V regulator inside the module. The 22 resistors shown are placed in series to protect SIM I/O port. The GSM part of WSN is protected against electro static discharge (ESD) with SMF05C, a 5 line transient voltage suppressor array, having a peak power dissipation of 100W (8 x 20 $\mu$S waveform) [7]. It has ESD rating of class 3B (exceeding 8 kV) per human body model and Class C (exceeding 400 V) per machine Model. Human body interaction with the circuitry is possible during SIM replacement.

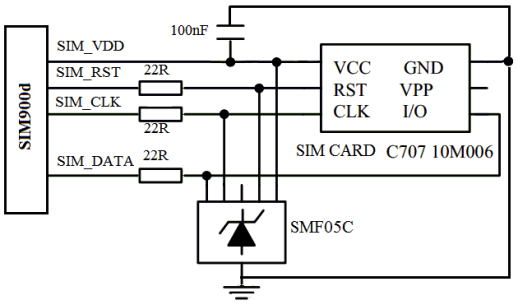


Fig. 4: SIM Card interface with GPRS module.

### D. Extreme Low Power Design

Today's applications should last for up to 5 to 10 years, while running from a single battery. To enable applications like these, we selected product of Microchip's PIC18F26K20 with sleep currents below 100 nA, watch-dog timer down to 1$\mu$A and run-currents down to 100 $\mu$A/MHz at 2.9V. We cannot use less than 4 MHz crystals, because then we will not be able to receive the sensor asynchronous TTL data at 9600 baud rate efficiently nor will we be able to read sensor's pulse width output of 1$\mu$ S/mm. Also, with 10 bit ADC resolution in the MCU, the resolution will always be less than 1mm. Hence we used 4MHz crystal with asynchronous TTL input from the sensor. We are powering the circuitry with 3.6V, 14,000mAH lithium thionyl chloride batteries with high surge currents.

GSM/GPRS transactions consume most of the battery power. We turn the GSM module off after every transaction

which takes 30uA at shutdown mode and is spending 99% of its time in this mode. Also, the sensors are turned on only at sampling time. The current consumed by ultrasonic and temperature sensors are negligible as compared to current consumed by the GPRS module.

### *E. Electronic Circuitry Protection*

The electronic circuitry is protected against harsh environmental conditions with IP67 (dust tight and protected against immersion) Ingress Protection standards die cast Aluminum Box. Die cast Aluminum is selected because it is not corroded even if immersed in water. To reduce signal attenuation inside the metal box, an external antenna is provided through IP67 standard connectors. The connectors are made of ABS plastic and are corrosion free with a special seal filled inside. We have tested WSN for IP67 [2] protection standards validity. We sealed the enclosure and placed it in water at 15cm below water level. We opened it after an hour; we observed water didn't diffuse inside the casing. Hence it fulfills temporary immersion casing standards.

## III. Design Problems and their solutions

After facing problems with weak signals in Bahawalnagar area, antenna poles were installed near the stilling well to get the highest possible signal strength. Being operated from 3.6V battery, we are quite close to the minimum voltage ratings of SIM900D i.e., 3.1V during burst. The copper traces from battery to the GSM module are 3.2 mm wide on top layer as well as on bottom layer in the PCB design to reduce the voltage drop in situations, where the circuit consumes high currents like 1-2A.

During assembling, anti-static wrist straps are used to prevent electrostatic discharge (ESD), by safely grounding the technician working with electronic equipment. It consists of a band of fabric with fine conductive fibers woven into it. Practical capacitors used in electric circuits are not ideal components with only capacitance. However they can be treated, to a very good degree of approximation, as being ideal capacitors in series with a resistance called equivalent series resistance (ESR). The ESR is mainly caused by the metallic resistance of the leads and electrodes and losses in the dielectric in a non-electrolytic capacitor or electrolytic capacitors with solid electrolyte. Capacitors are usually designed to minimize equivalent resistance. Under some circumstances, like we have to supply 1.5A current spike for 577$\mu$s of time, the resistance becomes important and even dominant. If our power supply cannot supply this amount of current during the spike, the GPRS module will never register itself with the network and no GPRS transaction will be possible. Aluminium and tantalum electrolytic capacitors with non-solid electrolyte have much higher ESR values, up to several ohms. A very serious problem, particularly with aluminium electrolytes, is that ESR increases over time with use; ESR can increase enough to cause circuit malfunction. Usually Capacitors of higher capacitance have lower ESR. Polymer capacitors usually have lower ESR than wet-electrolytic of same value and stable under varying temperature. Typical ESR values for 1000$\mu$F electrolytic capacitor is 0.12 Ohm, whereas for around the same value of Polymer capacitor the ESR value is 0.012 Ohm.

## IV. Performance

Refer to Fig. 5 below. The readings are taken measuring voltage across a 0.5 ohm precision resistor placed in series with WSN. So current readings in mA= 2* Voltage readings in mV. These plots are taken from Rigol DS1052E 50 MHz, 1GSa/sec digital oscilloscopes. We have these kinds of spikes during registration with the network, GPRS connectivity, connecting to the server and data transmission. The GSM signal quality as calculated by SIM900D was CSQ=18. Thus signal level in dBm= -113+2*18= -77dBm. In Fig. 5, a major grid on vertical axis=200mA whereas a major grid on horizontal axis= 20ms. Fig. 5 shows current spikes during sending the data to the server.

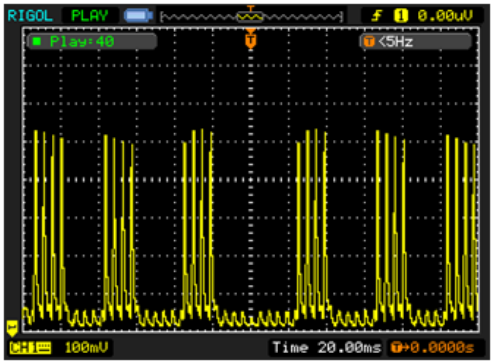

Fig. 5: Current vs. time plots during data transmission at -77 dBm.

Refer to Fig. 6 for the current spike of 1.45A scaled in time for another transaction with CSQ=12 (signal level in dBm= -113+2*12= -89dBm) and major grid on horizontal axis=2ms. The GSM/GPRS frame of 4.615ms time is divided into 8 equal time slots of 577$\mu$s each. As GSM/GPRS module transmits 1 time slot of 577 $\mu$s during a 4.615ms period, and receives or remains idle for the rest 4 ms time. Each Bit being 3.69231 $\mu$s long, only 114 data bits (total 156.25 bits) can be transmitted through 577 $\mu$s. For successful GPRS transaction, our battery should be capable of providing enough current to maintain this current without dropping the voltage below 3.1V at the peak. We connected two parallel 1200uF ultra low ESR capacitors across the battery terminals to provide sufficient current to continuous current spikes of around 1.5A.

Refer to Fig. 7, where we placed two ultra low ESR polymer capacitor 4SVP1200M (Made by SANYO) in parallel to ER34615M battery. There is not a question of 14000mAH only; we also need to make sure to use maximum percentage of this charge available. High capacitance across the battery ensures its full discharge. Each polymer capacitor has 12 milliohms ESR. Typical ESR values for electrolytic capacitors are greater than 120 milliohms, so we avoided using them. The battery internal resistance as approximated from manufacturer

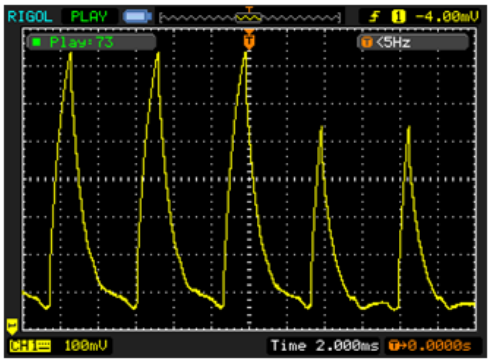


Fig. 6: Current vs. time plots during network registration at -89dBm.

specifications is 0.45 Ohm. For a current spike of 1.5A, we have RL=3.6/1.5= 2.4. Thus at high currents RL becomes comparable to battery internal resistance or ESR and we have a voltage divider. Now the GPRS module does not have enough power to transmit strong signal to communicate with the GSM tower.

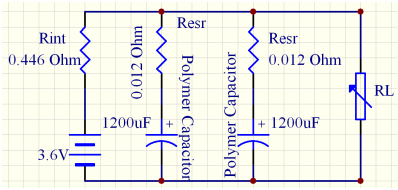


Fig. 7: Power module for WSN.

The GSM module transmits stronger signals in case of low signals to communicate control messages with the network. Refer to Fig. 8 for comparison between current vs. time plots for -73dBm and -93dBm signal levels. The later plot with -93dBm signal level has higher current spikes than with a signal level of -73dBm. Refer to Table I for more results. The major grid on horizontal axis represents 50 ms of time. As GSM/GPRS signals attenuate in metal casings, so we are using GPRS antenna external to the box for strong signals.

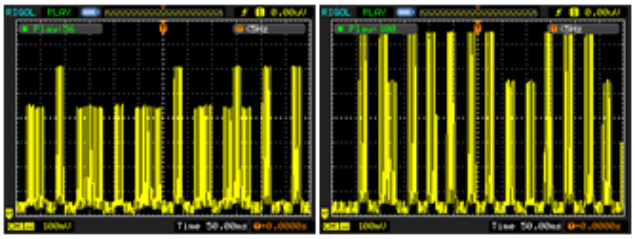

Fig. 8: Comparison of current vs. time plot for -73dBm and -93dBm signal levels.

We also tested WSN with Uni-Trend UT60A digital millimeter in the lab for three hours, with a 1 minute sampling interval of water level and 5 minutes of GPRS transmission interval. The average signal level at the lab was around -69dBm. We had a total of 37 GPRS tries and all of them successfully uploaded data to the server. We sampled the current every 0.5 second. The result for four GPRS transactions of the test is shown in the Fig. 9. To find the area under the curve for three hours (37 transactions),

$$q(T) = \int_0^T i(t)\,dt \approx \sum_{n=0}^{10800} i(n).\triangle t = 131.3 Coulomb.$$

which is 0.26 percent of the total charge available for single battery (14*60*60 C=50400 C). The small dot signs during sleep mode are currents consumed during sampling, when the sensors are active.

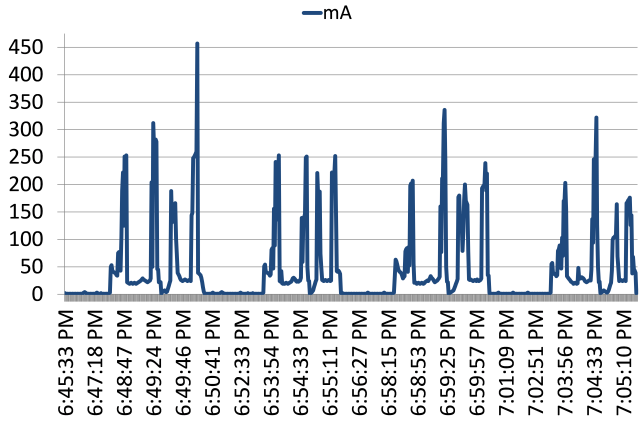


Fig. 9: Current Vs. Time plot for five transmission bursts.

An acrylic sheet calibration box with internal dimensions (width x length x depth=) 600mm x 600mm x 456mm was made. The water meter is calibrated for the range at which maximum accuracy is desired i.e., when there is normal water flowing in the distributary. This range is found to be between 400mm and 500mm. Therefore the instrument is calibrated for the range of 456mm. We calibrated 17 sensors and found out the sensor error was not more than 3mm for this range.

Refer to Fig. 10 for one year data of depth of flow data by a unit deployed at Bhagsen (5R) distributary, Distriict Bahawalnagar in Southern Punjab. See Fig. 11 for a photograph of the distributary and stilling well setting. Its design discharge is 37 cfs. The average signal level at test point was dBm= -113+2*22= -69dBm. The instrument was deployed on Aug 2nd, 2013 and still active at the time of updating of this paper (July 24, 2014) with a 10 minutes sampling interval and one hour transmission interval. We have recorded 48680 samples in total. Similar units have been deployed at 16 other sites at various distributories in Bahawalnagar since Dec 2014. Since this is the longest running unit, we summarize our observations below.

There are some missing readings. The insrument did not record data for one week from 3rd January, due to instrument malfunction and maintenance. Incidentally, the distributary was also shut down during this period due to annual canal closure

TABLE I: Average maximum current during burst for different signal levels

| Observation No. | Signal Quality, CSQ | Signal Strength | No. of bursts sampled with Oscilliscope | Average maximum current during burst |
|---|---|---|---|---|
| 1 | 27 | -59 dBm | 270 | 600mA |
| 2 | 20 | -73 dBm | 520 | 900mA |
| 3 | 18 | -77 dBm | 140 | 100mA |
| 4 | 10 | -93 dBm | 268 | 1450mA |

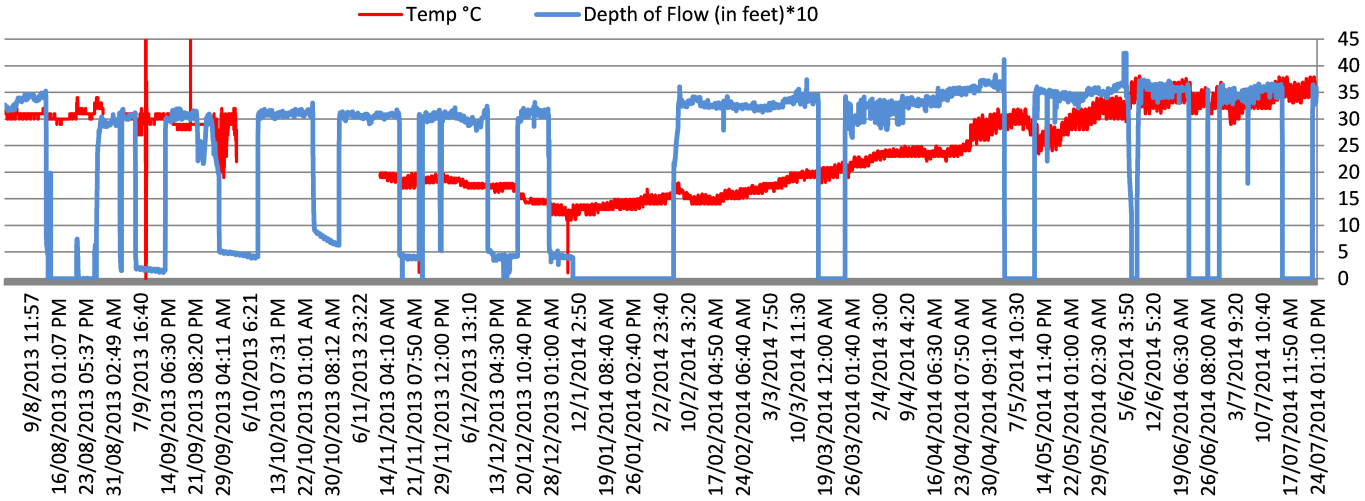


Fig. 10: One year data of a field deployed unit with 10 minutes sampling interval.

for maintenance. Therefore, there was no practical loss of data during this period. Similarly, we have three shorter periods of missing data (in hours) due to server failures or network operator problems. The frequency of these outages has gone down significantly after moving the server to cloud. The water temperature sensor malfunctioned for the period September 25 to November 10, 2013. This did not effect the calibration of the ultrasound unit since it uses another temperature sensor.

Fig. 11: Photograph of 5R distributary and stilling well.

The most interesting aspects of the recorded data are as follows. The data aligend with the announced canal closures by the irrigation department. Secondly, one can see the effects of silt deposition inside the stilling well at low flows. In the beginning, the low levels reported by the sensor during canal closure is close to zero. Progressively, this level is seen to be rising (e.g. the periods Auguest 14 to August 26; September 6 to September 13; September 28 to October 8; October 24 to November 1). During winter canal closure, the stilling well was cleaned which resulted in resetting the zero reading of the instrument at the right level.

Refer to Fig. 12 for another test of 4 days and 8 hours duration. The fixed water level was sampled every minute and transmitted every 10 minutes. Temperature varied between 17-45 degree C, whereas the water level only changed 15mm. The water level lowered during the four days slightly because of evaporation.

From Fig. 12 it is quite clear that we have on 15mm variation for 20 degree celcius change in temperature. The accuracy is due to the temperature compensation sensor, MB7955. We have compared the instrument reading with manual readings for data validation and got a good match at high flows. Refer to Fig. 13 for one such example. At low flows, the difference in levels reported manually and recorded electronically is due to silt accumulation and pooling of water at the bottom of the stilling well.

## V. Quality of Service

Refer to Fig. 14, Fig. 15 and Fig. 16 for the data outages at various distributaries. Distributary 1R has the minimum total outage of 3.5 hours followed by 9R with 6 hours outage over a period of 97 days. Distributary 3R has the most severe data loss of 568 hours, which is 24 percent of the recording period. The main Hakra branch canal was shut down for annual maintenance from Dec 20th, 2013 till Feb 6th, 2014 resulting in zero flows. Therefore, in the period following initial deployment, sensor and software failures were not addressed urgently

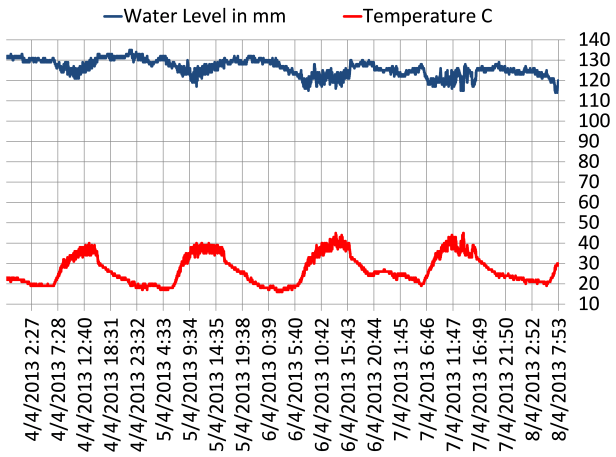


Fig. 12: Water level and temperature plot against time for a unit installed in a well designed for calibration with fixed water level.

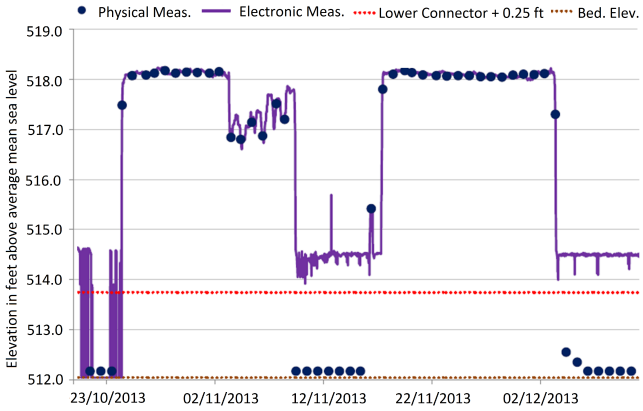


Fig. 13: Comparison between the instrument reading and daily physical measurements.

resulting in high data loss. After this period there was both a considerable increase in performance of sensors and decrease in data loss due to immediate maintenance. The server was shut down for 60 hours between March 8th, 2014 and March 10th, 2014 for a scheduled maintenance. All instruments recovered completely after server was back on-line with no data loss except 4R and 8R. The most severe failure occured with 3R, when the sensor developed hardware problems and recovery was not possible for 120 hours at a stretch despite repeated maintenance attempts.

These plots helped us identify some of the software bugs which occurs very rarely and were not noticed previously. Fig. 17 shows the percentage of data loss at each distributary, due to all types of failures. When a distributary is closed, the data loss is completely recoverable by an assumption of zero flow.

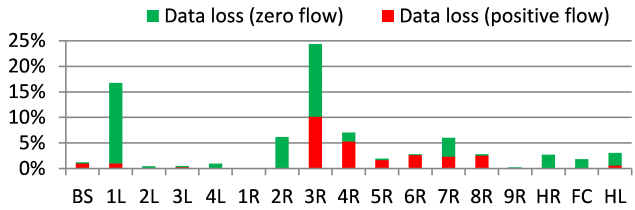


Fig. 17: Percentage of data loss at each distributary.

## VI. Conclusions

The results of various parameters shown in performance section, indicates that the designed hardware is a low power, field deployable and affordable for wide scale deployment in irrigation canal networks. Regarding the accuracy, we show that it achieves a practically acceptable limit in the field and is therefore, a feasible replacement of the current manual system. Power requirements, packaging, installation and system integration issues have been addressed and resolved.


## Acknowledgements

The authors would like to acknowledge financial support provided by the Embassy of the Kingdom of Netherlands, Islamabad, Pakistan through Grant #22294 used in part for the partnership between IWMI and LUMS to undertake the research described in this work.


## References


[1] EEMB; ER34615M. Lithium Thionyl Chloride Battery. "http://eemb.com, 2012.

[2] IEC 60529: Degrees of protection provided by enclosures (IP Code). International Electrotechnical Commission, Geneva.

[3] Maxbotix; MB7380 Outdoor Ultrasonic Range Finders. http://www.maxbotix.com, 2012.

[4] Microchip; PIC18F23K20/24K20/25K20/26K20/43K20/44K20/45K20/46K20 Data Sheet. 28/40/44-Pin Flash Microcontrollers with nanoWatt XLP Technology, 2010.

[5] Microchip; PIC18F26K20/46K20 Rev. B2/B3 Silicon/Data Sheet Errata, 2009.

[6] Nasir, H. and Muhammad A. Feedback Control of Very-Large Scale Irrigation Networks: A CPS Approach in a Developing-World Setting. 18th World Congress of International Federation of Automatic Control (IFAC), Milano, Italy, 2011.

[7] ON Semiconductor; SMF05C Transient Voltage Suppressors. http://onsemi.com, 2005.

[8] SIMCOM; SIM900D GSM/GPRS Module Hardware Design Manual V1.03. www.sim.com, 2010.

[9] Tariq M. U., Nasir H., Muhammad A. and Wolf M. Model-Driven Performance Analysis of Large Scale Irrigation Networks. IEEE/ACM International Conference on Cyber-Physical Systems (ICCPS), Beijing, China, 2012.

[10] The Corporate Technical Journal, Growing Smart Solutions with Irrigation, www.abb.com/water, 2009.

[11] Zahoor Ahmad, Ehsan U. Asad, Abubark Muhammad, Waqas Ahmad and Arif Anwar. Development of Low-Power Smart Water Meter for Discharges in Indus Basin Irrigation Network. 1st International Conference on Wireless Sensors Networks for Developing Countries (WSN4DC), Jamshoro, Pakistan, 2013.

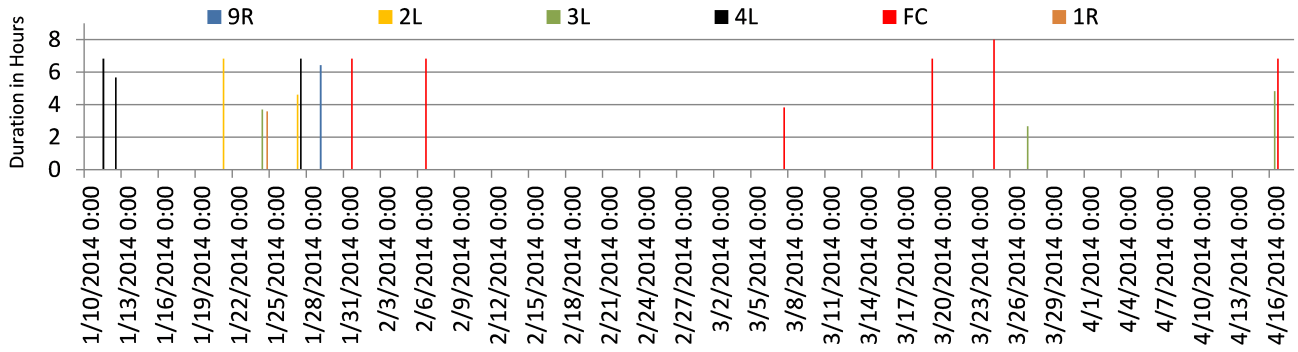


Fig. 14: Data losses (in hours) for distributaries with short names 9R, 2L, 3L, 4L, FC and 1R.

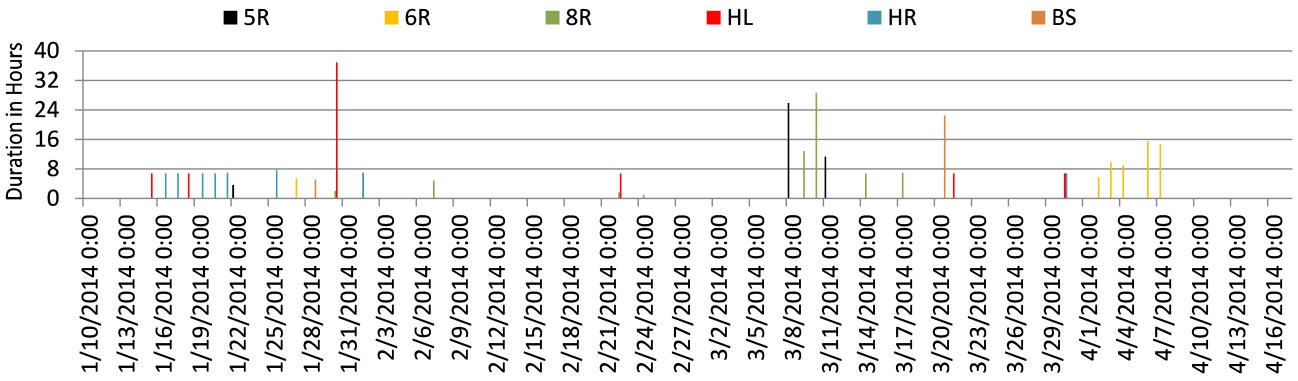


Fig. 15: Data losses (in hours) for distributaries with short names 5R, 6R, 8R, HL, HR and BS.

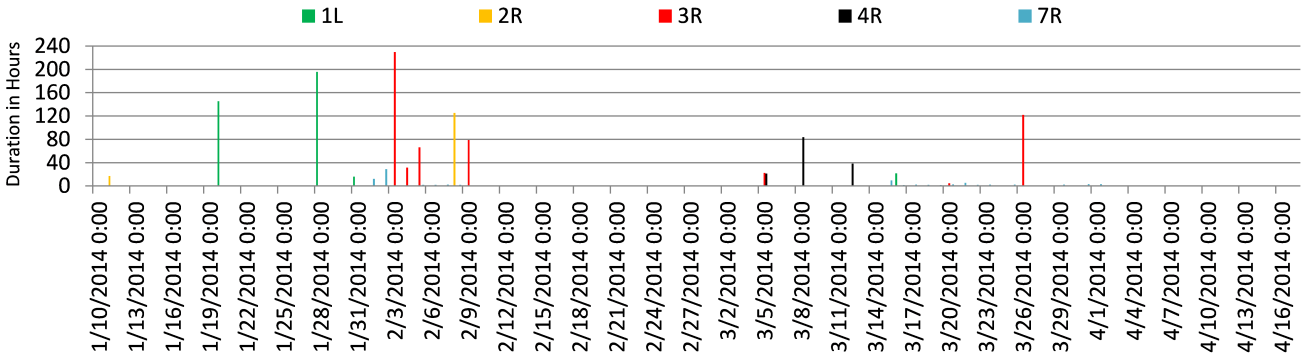


Fig. 16: Data losses (in hours) for distributaries with short names 1L, 2R, 3R, 4R and 7R.